SCIENTIFIC REPORTS

OPEN

SUBJECT AREAS:
METALS AND ALLOYS
ELECTRONIC PROPERTIES AND MATERIALS
MAGNETIC PROPERTIES AND MATERIALS
INFORMATION STORAGE

Received
18 July 2012

Accepted
5 October 2012

Published
19 October 2012

Correspondence and requests for materials should be addressed to H.L. (h.li@fz-juelich.de)

Possible magnetic-polaron-switched positive and negative magnetoresistance in the GdSi single crystals

Haifeng Li[1,2], Yinguo Xiao[3], Berthold Schmitz[3], Jörg Persson[3], Wolfgang Schmidt[1], Paul Meuffels[4], Georg Roth[2] & Thomas Brückel[3]

[1]Jülich Centre for Neutron Science JCNS, Forschungszentrum Jülich GmbH, Outstation at Institut Laue-Langevin, Boîte Postale 156, F-38042 Grenoble Cedex 9, France, [2]Institut für Kristallographie der RWTH Aachen University, D-52056 Aachen, Germany, [3]Jülich Centre for Neutron Science JCNS and Peter Grünberg Institut PGI, JARA-FIT, Forschungszentrum Jülich GmbH, D-52425 Jülich, Germany, [4]Peter Grünberg Institut PGI and JARA-FIT, Forschungszentrum Jülich GmbH, D-52425 Jülich, Germany.

Magnetoresistance (MR) has attracted tremendous attention for possible technological applications. Understanding the role of magnetism in manipulating MR may in turn steer the searching for new applicable MR materials. Here we show that antiferromagnetic (AFM) GdSi metal displays an anisotropic positive MR value (PMRV), up to ~415%, accompanied by a large negative thermal volume expansion (NTVE). Around T_N the PMRV translates to negative, down to ~−10.5%. Their theory-breaking magnetic-field dependencies [PMRV: dominantly linear; negative MR value (NMRV): quadratic] and the unusual NTVE indicate that PMRV is induced by the formation of magnetic polarons in 5*d* bands, whereas NMRV is possibly due to abated electron-spin scattering resulting from magnetic-field-aligned local 4*f* spins. Our results may open up a new avenue of searching for giant MR materials by suppressing the AFM transition temperature, opposite the case in manganites, and provide a promising approach to novel magnetic and electric devices.

Magnetoresistance (MR), a change in electrical resistivity when an external magnetic field ($\mu_0 H$) applied, occurs in metals, inorganic and organic semiconductors, and particularly close to an intermediate regime of the transformations of charge (insulator, metal) order and spin [paramagnetic (PM), ferromagnetic (FM)] order in thin manganites' films as a colossal negative MR value (NMRV)[1–5]. The colossal MR (CMR) in manganites is accompanied by a shift of the transition temperature to a higher value by applied magnetic field so that a sharp peak appears in the MR values near the transition, e.g., the NMRV reaches ~−95% at $\mu_0 H = 15$ T near $T_c = 240$ K in $La_{0.85}Sr_{0.15}MnO_3$[6]. Although the double exchange interaction can qualitatively explain the CMR effect based only on the charge and spin degrees of freedom, the exact picture still remains elusive.

We investigate here the intermetallic GdSi that crystallizes in the FeB-type structure (*Pnma*) and orders antiferromagnetically below ~55 K[7–11]. The vanished orbital momentum ($L = 0$) naturally removes the crystal electric field (CEF) as well as its perturbation on magnetic interactions, which renders GdSi ideal for studying pure spin-magnetism-tuned transport. Meanwhile, there keep solely two main sources for the magnetovolume (MV) effect. One contribution is from the volume dependence of the Ruderman-Kittel-Kasuya-Yosida (RKKY) exchanges, which normally produces a negative MV (NMV) effect. The other is due to the spin-polarized itinerant moments in the conduction bands, resulting in a positive MV (PMV) effect. Therefore, the volume variation (NMV or PMV) with temperature in a magnetic state could be useful in determining the nature of its magnetic origin. Even after nearly 50 years of research on GdSi[8–11], to our knowledge, there is little data on its temperature-dependent structural modifications and MR property. Here we report on detailed temperature-dependent powder diffraction, angular-dependent magnetic characteristic and transport studies of GdSi single crystals. We find anomalous anisotropic giant MR and spontaneous magnetostriction (MS) effects, in particular, an antiferromagnetic (AFM)-driven negative thermal volume expansion (NTVE) and a nontrivial positive to negative MR transition, which can be well understood by combining the magnetic tunnel of conduction electrons and the concept of magnetic polarons[12], i.e., local short-range FM spin regimes[12].

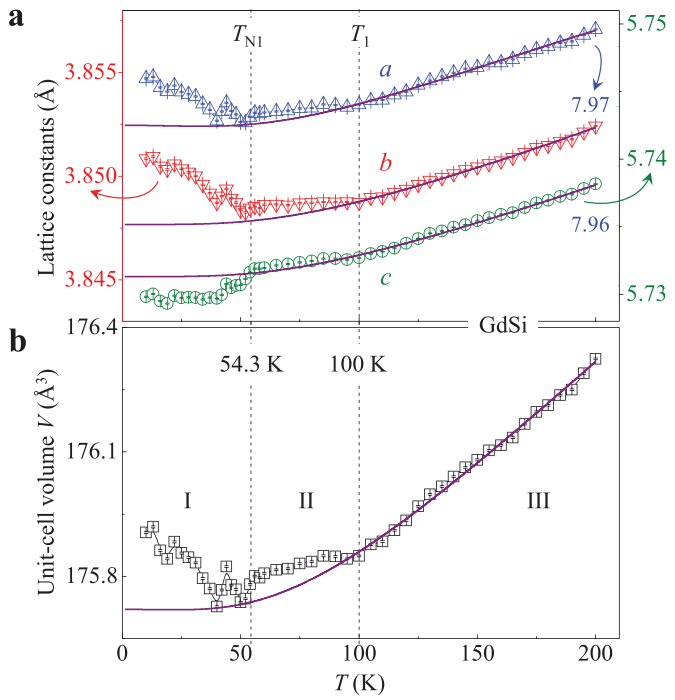

Figure 1 | Temperature-dependent structural parameters. (a) Anisotropic character of the lattice-constants, *a, b* and *c*, variation. (b) Anomalous unit-cell volume, *V*, expansion with temperature in the *Pnma* symmetry. The solid lines are theoretical estimates of the temperature-dependent structural parameters using the Grüneisen model with Debye temperature of θ_D = 340 K, which is the same as reported in Ref. [10]. Upon warming, two appreciable anomalies display in the structural parameters at respective temperatures of $T_{N1} \approx 54.3$ K (at 0.06 T) and $T_1 \approx 100$ K. Error bars in (a) and (b) are the standard deviation obtained from the Fullprof refinements.

Results

Structural studies. The x-ray powder diffraction analysis (Fig. 1) clearly shows three distinct structural regimes (I, II and III). Upon cooling, the refined (Re) *a, b, c* and *V* shrink almost linearly before T_1, followed by a slower decrease until sharp turns at T_{N1}, an onset temperature of the AFM transition. Below T_{N1}, the increases of *a* and *b* and the decrease of *c* ultimately result in an unusual NTVE (i.e., PMV) in the unit-cell volume *V*, which is quite useful in fabricating applicable materials with controlled thermal expansion values[13,14]. Obviously broadening in the nuclear Bragg peaks is present in the I regime (see Supplementary Fig. S1b), which is attributed to the magnetoelastic effect (the coupling between magnetic moments and lattice strains). The strain distribution patterns are extracted and shown in Supplementary Fig. S2. The variations in *a, b, c* and *V* below T_{N1} imply that magnetic anisotropy (MA) (which is consistent with Supplementary Fig. S3a and uncommon for the *S*-state Gd-compounds), spontaneous PMV and anisotropic MS effects exist in GdSi.

The CEF is mainly responsible for the giant MS effect in rare-earth (RE) compounds. This effect is thus expected to be negligible in GdSi. However, below T_1, structural parameters shown in Fig. 1a obviously deviate from the theoretical estimates (solid lines) by the Grüneisen (Gr) law, e.g., $\frac{a_{Re}^{10K}-a_{Gr}^{10K}}{a_{Gr}^{10K}} = 4.94(6)\times10^{-4}$, $\frac{b_{Re}^{10K}-b_{Gr}^{10K}}{b_{Gr}^{10K}} = 8.24(9)\times10^{-4}$ and $\frac{c_{Re}^{10K}-c_{Gr}^{10K}}{c_{Gr}^{10K}} = -2.60(8)\times10^{-4}$, denoting large anisotropic spontaneous MS effects. The formation of long-range-ordered (LRO) AFM state is a process of the growth of sublattice FM domains. The enlargement of FM domain volumes with decreasing temperature may accumulate strains on the domain walls, which is the microscopic mechanism for the magnetic-field-induced MS effect in ferromagnets. Therefore, including the effect of the molecular field of one Gd-AFM-sublattice on the other is indispensable to understand the *spontaneous* MS effect in GdSi. According to the Stoner model for itinerant magnetic electrons, the positive magnetic pressure P_M associated with the magnetic ordering in a band is proportional to $\frac{\partial \ln D}{\partial \ln V}M^2$, where *D, V* and *M* represent the electronic density of states at the Fermi energy, the volume and the magnetic moment, respectively. The spontaneous PMV effect (i.e., NTVE), e.g., $\frac{V_{Re}^{10K}-V_{Gr}^{10K}}{V_{Gr}^{10K}} = 1.04(2)\times10^{-3}$, is therefore attributed mainly to the increases of *D* (corresponding to the pronounced decrease of ρ below T_N in Fig. 2a) and the induced itinerate spin-moments in conduction bands. Similar MS and MV effects were also reported in Gd_3Ni[15], where, however, they are ascribed to the itinerant character of the Ni 3*d* bands.

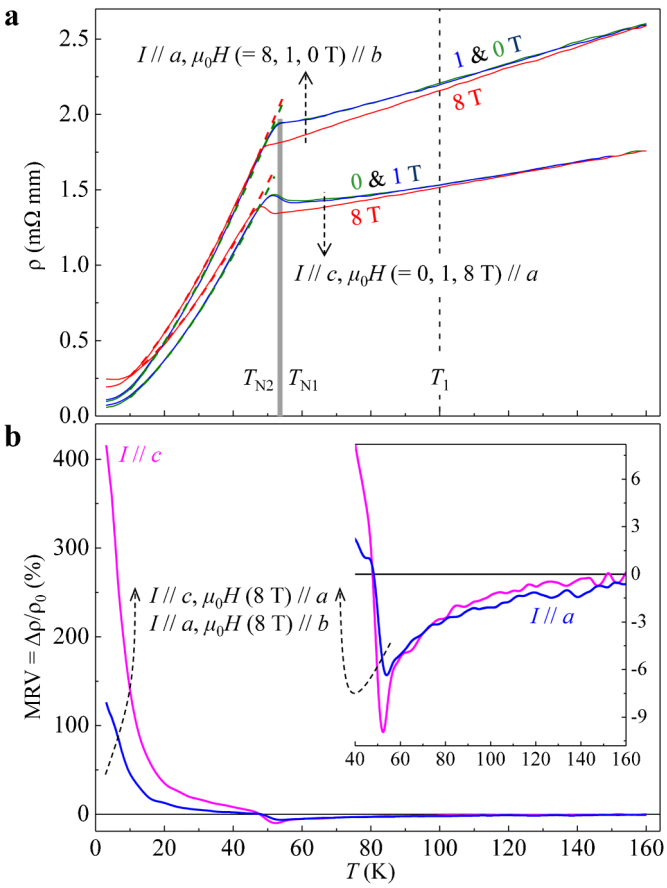

Figure 2 | Temperature variations of resistivity and MR effect. (a) Resistivity measurements with current *I* along the *a* and *c* axes under applied magnetic fields of 0, 1 and 8 T. T_1 = 100 K labels the temperature where one structural anomaly occurs as shown in Fig. 1 . The dashed lines are fits between 10 K and 40 K (details in text), and extrapolated to higher temperatures. (b) Corresponding MR values versus temperature. The MR effect along the *a* axis has a similar trend to that of the *c* axis albeit with a lower value. The positive MR values decrease sharply with increasing temperature below ~20 K, then gradually transfer into negative around T_N, and persist up to ~120 K. By contrast, in amorphous Gd_xSi_{1-x} films, only the NMRV was observed[16–18] near the metal-insulator transition. In (a), there is no big difference for the data at 0 and 1 T above ~20 K. The solid lines in (a) and (b) in the dashed arrow direction in turn correspond to the ordinal axis-direction and applied magnetic-field strength as labeled, respectively.

Resistivity measurements. As depicted in Fig. 2a, the zero-field-cooling (ZFC) electrical resistivity at 0 T with current I along the a and c axes decreases linearly due to the weakened thermal excitations upon cooling until around T_N (vertical bar), where a hump with negative slop appears along only the c axis, probably attributed to the magnetic superzone effect[19] as a consequence of the AFM ordering. Below T_N, they decrease steeply like a reasonable AFM metal. The resistivity between 10 K and 40 K[20] can be well fit to $\rho(T) = \rho_0 + kT^w$, shown as dashed lines. This produces $w^{c,0T} = 1.51(2)$, $w^{c,8T} = 1.56(4)$, $w^{a,0T} = 1.43(2)$ and $w^{a,8T} = 1.51(1)$. All w values are much smaller than 5[20] indicative of anisotropic magnetic interactions.

Anisotropic MR effect and positive MR value (PMRV) to NMRV transition. The most intriguing results from resistivity measurements are the anisotropic MR effect (Figs 2b, 3 and 4) and the existence of both positive and negative MR values, up to ~415% (comparable to the CMR value in manganites[1,6] and one to two orders of magnitude larger than that of the RE-metals[21]) and down to ~−10.5% along the c axis at 8 T and 3 K and 52.8 K, respectively. The MR anisotropy in the ac and bc plans is shown in Fig. 3. They display a twofold symmetry at 7K (Figs 3a and 3d). We notice that applied magnetic field of 8 T does not suppress (produce) the (a) hump along the c and a axes, respectively, near T_N, and the MR twofold symmetry is persistent from 1 to 8 T, indicating that applied magnetic field in a strength of 8 T may just align or localize the 5d moments, and slightly rotate and tilt the 4f moments while conserving the superzone energy gap. Therefore, the MR effect in GdSi exhibits a well separate feature of the temperature regions for the positive and the negative MR values (Fig. 2b), respectively, which is induced jointly by the AFM superzone effect[19] and the shift of the AFM transition to lower temperatures in external applied magnetic field analogous to the case in manganites[1,2,6]. For metals, mean-field theories predict that spin fluctuations induced by applied magnetic field from the localized magnetism produce a PMRV with the quadratic-field dependence in antiferromagnets, whereas a NMRV with the linear variation in ferromagnets and paramagnets[22]. However, in GdSi, the PMRV in the AFM state mainly displays a linear magnetic-field dependence (Figs 4a and 4c), while above T_{N1} the absolute NMRV is proportional to the square of the strength of applied magnetic field (Figs 4b and 4d). Both the positive and negative MR effects do not saturate at utilized maximum $\mu_0 H$ = 8 T (Fig. 4). In addition, the ratio of the resistivity at 160 K and 7 K in Fig. 2a is already ~12–25, therefore, the cyclotron motion of the conduction electrons could be neglected at $\mu_0 H$ = 8 T (i.e., $\omega_c \tau \ll 1$, where ω_c is the cyclotron frequency and τ is the life time of the conduction electrons). Therefore, these uncommon magnetic-field variations indicate new transport mechanisms for the MR effects of GdSi.

Discussion

In GdSi, the conduction electrons (mainly 5d bands) are different from those responsible for the magnetism (4f component plus possible part of the 5d component). The former is normally delocalized, acting as the magnetic glue among magnetic ions (Fig. 5), and scattered by them, leading to electrical resistance. The magnetism from the 4f part is generally localized with weak interactions. Therefore,

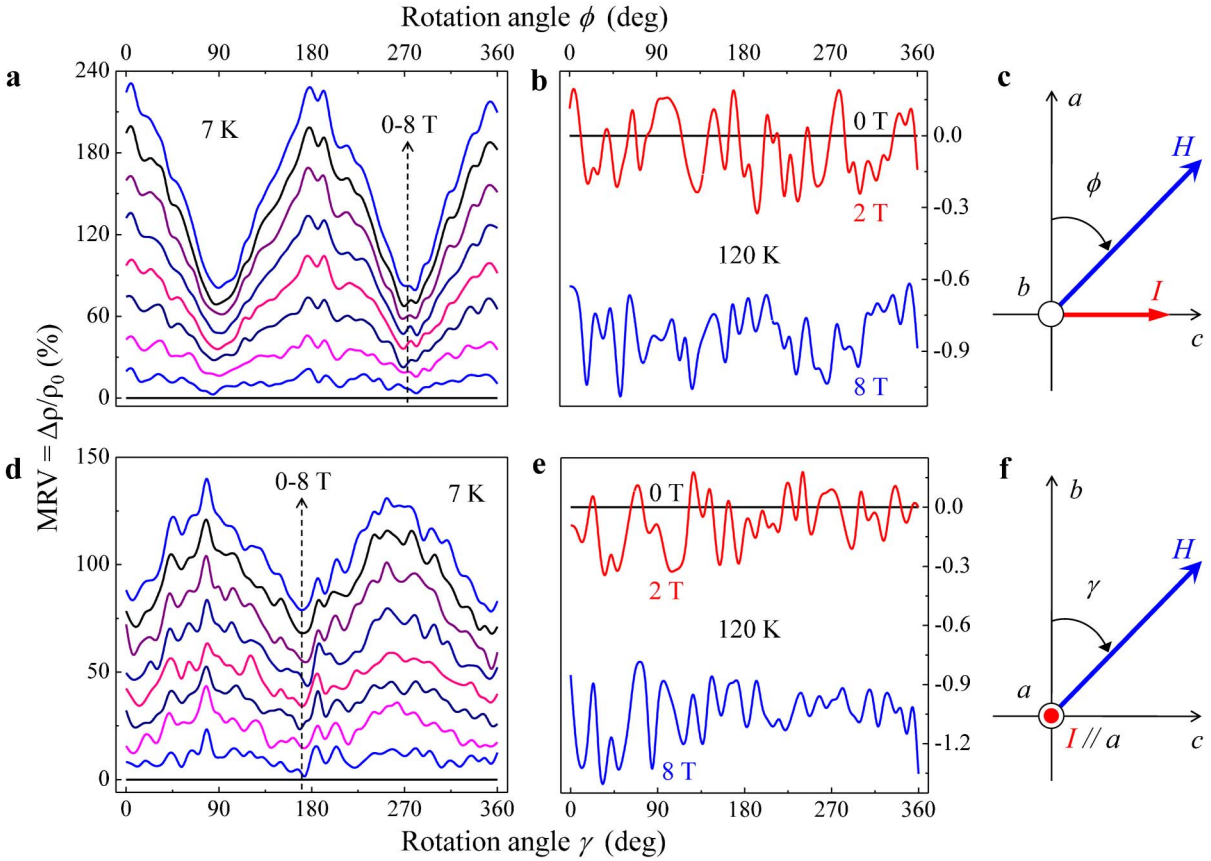

Figure 3 | Angular-dependent MR values under different applied magnetic fields. (a) Angular-dependent MR values with applied magnetic field in a range of 0 to 8 T (1 T step) at 7 K, and (b) at 120 K (0, 2 and 8 T). (c) For (a) and (b) measurements, current I is along the crystallographic c axis, and applied magnetic field, $\mu_0 H$, rotates away from the a axis with an angle of ϕ in the ac plane. (d) Angular-dependent MR values with applied magnetic field in a range of 0 to 8 T (1 T step) at 7 K, and (e) at 120 K (0, 2 and 8 T). (f) For (d) and (e) measurements, $I \| a$-axis and applied magnetic field, $\mu_0 H$, rotates in the bc plane with an angle of γ deviated from the b axis.

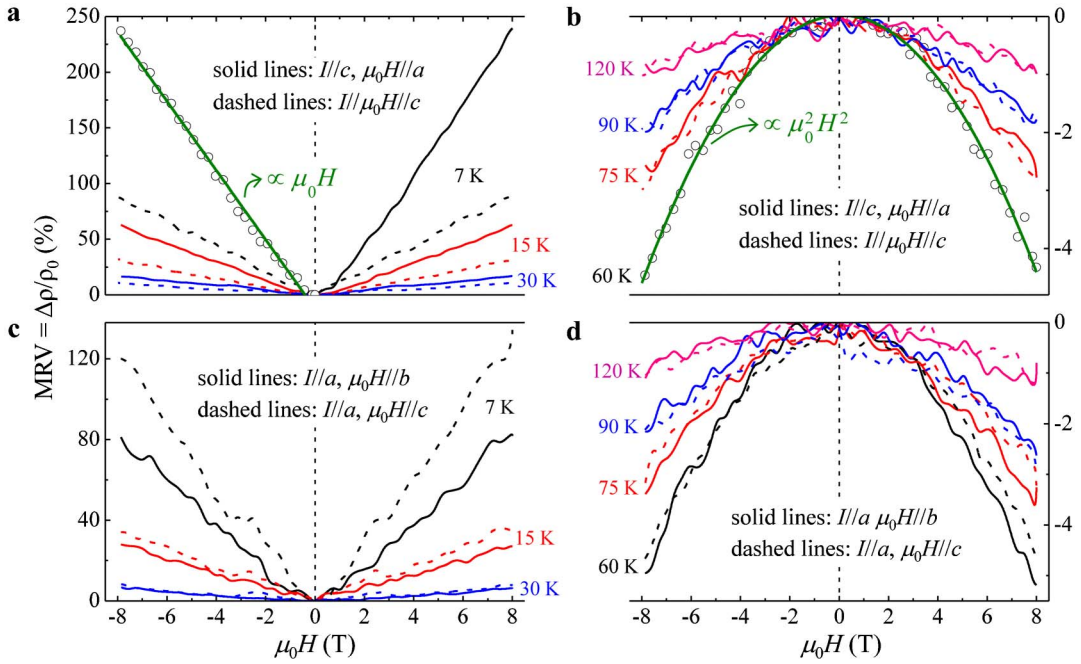

Figure 4 | Field- and temperature- dependent MR values. (a) Field and temperature dependencies of the MR values with $I \| c$-axis and applied magnetic field, $\mu_0 H$, along the a or c axis below T_N, and (b) above T_N. The representatives of the linear-field dependence of the PMRV (i.e., the PMRV is proportional to the strength of applied magnetic field) at 7 K (blow T_N) and the quadratic variation of the NMRV (i.e., the absolute NMRV is proportional to the square of the strength of applied magnetic field) at 60 K (above T_N) were shown in (a) and (b), respectively. (c) Field and temperature dependencies of the MR values with $I \| a$-axis and applied magnetic field, $\mu_0 H$, along the b or c axis below T_N, and (d) above T_N.

the LRO AFM state originates mainly from the isotropic RKKY interactions through conduction bands[23]. The interaction between localized moments, $\vec{M}_{loc}$, and itinerant ones, $\vec{m}_{iti}$, can generate an extraordinarily large Zeeman splitting in the mean-field approximation[24]

$$E = g^* \mu_B \vec{m}_{iti} \cdot H + 2J(H) \vec{m}_{iti} \cdot \left\langle \vec{M}_{loc} \right\rangle, \quad (1)$$

where g^* is the spectroscopic splitting factors for the carriers, μ_B is the Bohr magneton, J is the effective exchange coefficient and

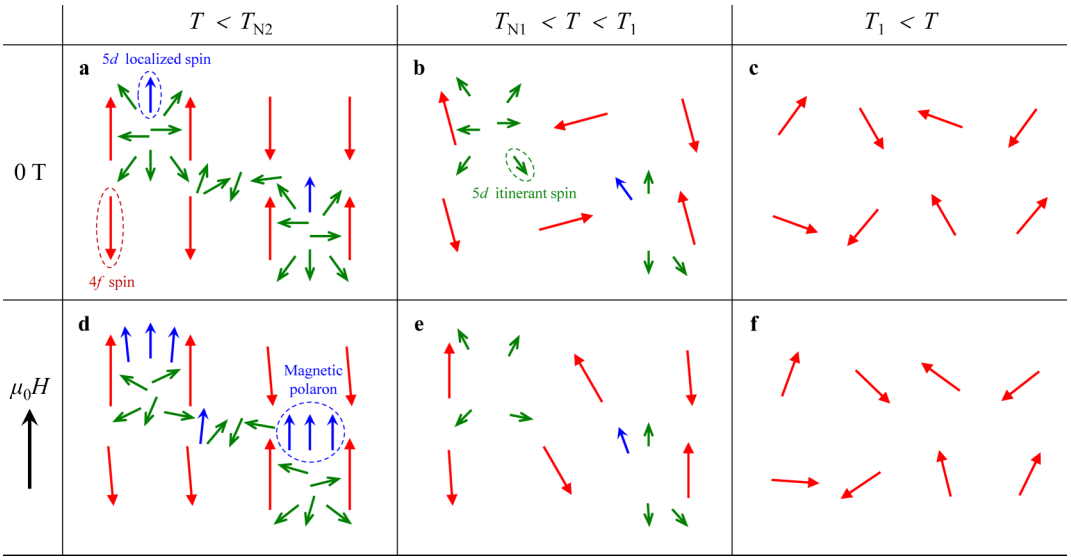

Figure 5 | Schematic illustration of the spin states with and without applied magnetic field, $\mu_0 H$, in different temperature regimes. (a–c) At zero magnetic field. (d–f) At applied magnetic field of $\mu_0 H$. When $T > T_1$, spin moments more or less rotate (f), depending on the strength of $\mu_0 H$ and the size of MA, from a pure PA state (that is strictly observing the Curie-Weiss law as shown in Supplementary Fig. S4) in (c). When $T_{N1} < T < T_1$, the short-range AFM spins that are attributed only to the local 4f moments appear (b) accompanied by the generations of polarized itinerate 5d spins, based on the deviation of the unit-cell volume from the Grüneisen model shown in Fig. 1b, and possible small amount of localized 5d spins according to equation (1). Applied magnetic field mainly aligns the local AFM spins (e), leading to a decrease of the electron-spin scattering and resultant the NMRV. When $T < T_{N2}$, the LRO AFM state with almost equivalent AFM and FM interactions (see Supplementary Fig. S4) forms (a) with more itinerate 5d moments (based on the large PMV effect shown in Fig. 1b). Applied magnetic field mainly localizes more 5d moments by enhancing the exchange of J in equation (1), resulting in the formation of magnetic polarons and the consequent PMRV (d).

$\langle\overrightarrow{M}_{loc}\rangle$ is the averaged local moment in the regime of band electrons. Since $\overrightarrow{m}_{iti}$ is usually small, and the second term could be very large (e.g., amounting to fractions of an eV in the LRO magnetic state of Eu-compounds[24]), in addition, J is strongly associated with applied magnetic field by virtue of modifying spin fluctuations of $\overrightarrow{M}_{loc}$, the formation of magnetic polarons in the 5*d* bands by this splitting in the LRO AFM state of GdSi is thus possible. Therefore, when $T < T_{N2}$, the modified J at 8 T drives some of the conducting moments (as foregoing remarks) to form local magnetic polarons that lead to a largely degenerate conduction (i.e., PMRV) (Figs 5a and 5b). In this case, the more extended 5*d* bands almost certainly offer a small FM component, which dominates the linear-magnetic-field dependence below T_{N2}.

Above T_{N1}, the LRO AFM 4*f* moments disappear, which is implied by the change of the χ relationship between the *a, b* and *c* axes (see Supplementary Fig. S3a). However, the upward deviation of $1/\chi$ from the Curie-Weiss law below T_1 (see Supplementary Fig. S4) along with the concomitant anomalous volume lattice distortions (Fig. 1) indicates that a kind of striking AFM state exists there, which can be ascribed only to the local short-range AFM 4*f* moments (Fig. 5b) according to equation (1) (broad 5*d* states indeed could not form a magnetic state by themselves). This local AFM state theoretically[22] leads to the quadratic-magnetic-field variation (Figs 4b and 4d). The local AFM moments above T_{N1} are possibly oriented irregularly in the PM state and become compulsorily aligned and to some extent spin-tilted (Fig. 5e), leading to the decrease in resistivity and thereby promoting a NMRV.

Including the contribution of magnetic polarons into the mean-field approximation of the MR effect of AFM metals[22,25–27], the MR value (MRV) then equals

$$\begin{aligned}|\mathrm{MRV}| &\approx A\left|\overrightarrow{M}_{In}^{4f}+\overrightarrow{M}_{In}^{5d}\right|^2 \\ &\approx A\left(\left|\overrightarrow{M}_{In}^{4f}\right|^2+2\left|\overrightarrow{M}_{In}^{4f}\right|\left|\overrightarrow{M}_{In}^{5d}\right|\cos\alpha+\left|\overrightarrow{M}_{In}^{5d}\right|^2\right),\end{aligned} \quad (2)$$

where A is a constant, M_{In} is the induced local magnetization by applied magnetic field, $\mu_0 H$, α is the angle between $\overrightarrow{M}_{In}^{4f}$ and $\overrightarrow{M}_{In}^{5d}$, $\overrightarrow{M}_{In}^{4f}=\overrightarrow{\chi}_{In}^{4f}\mu_0 H$, and $\overrightarrow{\chi}_{In}^{4f}$ is the magnetic susceptibility of the 4*f* site along the AFM sublattice direction. At $T_{N1} < T < T_1$, neglecting $\left|\overrightarrow{M}_{In}^{5d}\right|$, $|\mathrm{NMRV}| \propto \left|\overrightarrow{M}_{In}^{4f}\right|^2=\left|\overrightarrow{\chi}_{In}^{4f}\right|^2\mu_0^2H^2$, resulting in a quadratic-magnetic-field dependence. At $T < T_{N2}$, in our case, the linear part in equation (2) is dominate, i.e., $\mathrm{PMRV}\propto\left|\overrightarrow{M}_{In}^{4f}\right|\left|\overrightarrow{M}_{In}^{5d}\right|\cos\alpha=\left|\overrightarrow{\chi}_{In}^{4f}\right|\left|\overrightarrow{M}_{In}^{5d}\right|\mu_0 H\cos\alpha$, which produces not only the linear-magnetic-field dependence but also the twofold MR symmetry (Figs 3a and 3d). Quantitative analysis requires the knowledge of the exact directions of $\overrightarrow{\chi}_{In}^{4f}$ and $\overrightarrow{M}_{In}^{5d}$. The involvement of magnetic polarons in understanding the MR effects here is further supported by the existence of strong FM Gd-Gd interactions (see Supplementary Fig. S4).

RE 4*f* electrons generally remain localized so that their properties in an alloy closely resemble those in the single-elemental metals. It is therefore interesting to compare the microscopic conducting mechanism of GdSi with that of the 3*d* transition metals[28,29]. Roughly, the 4*f* shells highly screened by the 5*s* and 5*p* states are better shielded than the transition metal (TM) 3*d* ones. Therefore, the 4*f* electrons are well embedded within the atom, and the 5*d* and 6*s* states act as conduction electrons in the metals, though band structure calculations suggested that the upper part of the 4*f* spin minority may hybridize with the unoccupied 5*d* and 6*s* bands[30]. On the contrary, for 3*d* TMs, the conductivity is mainly dominated by the *s-s* and *d-d* transitions at low temperatures, in addition to the *s-d* transitions (increasing the effective electron mass and shortening the mean free path) at high temperatures[28,29], supposing that both *s* and *d* electrons are conduction electrons. Since almost all RE 4*f* metals and only some of the 3*d* TMs (Fe, Co, Ni and Mn) order magnetically at low temperatures, magnetism plays a more crucial role in controlling electrical property of RE 4*f* metals.

In summary, GdSi displays a wide array of novel behaviors including a two-step AFM transition, an anisotropic spontaneous MS effect, magnetostrictive strains, in particular, an exotic NTVE (spontaneous PMV) and a peculiar positive to negative MR transition, indicating a strong coupling between spin, lattice and charge degrees of freedom. The peculiar PMRV to NMRV transition and their non-trivial[22] magnetic-field dependencies are predominated by the nature of the 4*f* moments and the polaronic 5*d* carriers. Coexistence of these extraordinary behaviors in the same Gd-compound is unique. The present results make GdSi an fascinating system for theoretical and further experimental explorations.

Methods

Since the neutral Gd is a strong thermal neutron absorber, we therefore performed a powder x-ray diffraction study of the pulverized GdSi single crystal on an in-house diffractometer employing the copper $K_{\alpha 1}$ = 1.5406(9) Å as the radiation with a 2θ step size of 0.005° from 10 to 300 K to explore the temperature-dependent structural modifications. X-ray powder diffraction data were analyzed by Fullprof suite[31]. ZFC dc magnetization (M) measurements were performed on a Quantum Design MPMS-7 superconducting quantum interference device (SQUID) magnetometer. The ZFC electrical resistivity (ρ) of bar-shaped ($\sim 0.6 \times 1 \times 6$ mm^3) single crystals was measured by standard DC four-probe technique using a commercial physical property measurement system (PPMS), equipped with the option of rotating the sample *in situ*. Commercial silver paint and 25 μm gold wire were used for electrical contacts. $\mathrm{MRV}(\mu_0 H,T,\phi/\gamma)=\frac{\rho(\mu_0 H,T,\phi/\gamma)-\rho(0,T,\phi/\gamma)}{\rho(0,T,\phi/\gamma)}\times 100\%$, where $\rho(\mu_0 H, T, \phi/\gamma)$ and $\rho(0, T, \phi/\gamma)$ are the resistivity with and without $\mu_0 H$ at a given temperature, T, and a rotating angle of ϕ or γ (Figs 3c and 3f).

1. Van Santen, J. H. & Jonker, G. H. Electrical conductivity of ferromagnetic compounds of manganese with perovskite structure. *Physica* **16**, 599–600 (1950).
2. Jin, S., Tiefel, T. H., McCormack, M., Fastnacht, R. A., Ramesh, R. & Chen, L. H. Thousandfold change in resistivity in magnetoresistive La-Ca-Mn-O films. *Science* **264**, 413–415 (1994).
3. Shimakawa, Y., Kubo, Y. & Manako, T. Giant magnetoresistance in $Tl_2Mn_2O_7$ with the pyrochlore structure. *Nature* **379**, 53–55 (1996).
4. Majumdar, P. & Littlewood, P. B. Dependence of magnetoresistivity on charge-carrier density in metallic ferromagnets and doped magnetic semiconductors. *Nature* **395**, 479–481 (1998).
5. Xiong, Z. H., Wu, D., Valy Vardeny, Z. & Shi, J. Giant magnetoresistance in organic spin-valves. *Nature* **427**, 821–824 (2004).
6. Urushibara, A., Moritomo, Y., Arima, T., Asamitsu, A., Kido, G. & Tokura, Y. Insulator-metal transition and giant magnetoresistance in $La_{1-x}Sr_xMnO_3$. *Phys. Rev. B* **51**, 14103–14109 (1995).
7. Gladyshevskii, E. I. & Kripyakevich, P. I. Monosilicides of rare-earth metals and their crystal structures. *Zh. Strukt. Khim* **5**, 853–859 (1964).
8. Nagaki, D. A. & Simon, A. Structure of gadolinium monosilicide. *Acta Cryst* **C46**, 1197–1199 (1990).
9. Saito, H., Suzuki, S., Fukamichi, K., Mitamura, H. & Goto, T. Metamagnetic transition in GdSi. *J. Phys. Soc. Jpn* **65**, 1938–1940 (1996).
10. Tung, L. D., Lees, M. R., Balakrishnan, G., Paul, D., Mc, K., Schobinger-Papamantellos, P., Tegus, O., Brommer, P. E. & Buschow, K. H. J. Field-induced magnetic phase transitions in a GdSi single crystal. *Phys. Rev. B* **71**, 144410–4 (2005).
11. Roger, J., Babizhetskyy, V., Hiebl, K., Halet, J.-F. & Guérin, R. Structural chemistry, magnetism and electrical properties of binary Gd silicides and Ho_3Si_4. *J. Alloys Compd* **407**, 25–35 (2006).
12. Heikes, R. R. & Chen, C. W. Evidence for impurity bands in La-doped EuS. *Physics*, **1**, 159–160 (1964).
13. Barrera, G. D., Bruno, J. A. O., Barron, T. H. K. & Allan, N. L. Negative thermal expansion. *J. Phys. Condens. Matter* **17**, R217–R252 (2005).
14. Ibarra, M. R., Algarabel, P. A., Marquina, C., Blasco, J. & García, J. Large magnetovolume effect in yttrium doped La-Ca-Mn-O perovskite. *Phys. Rev. Lett* **75**, 3541–3544 (1995).
15. Kusz, J., Böhm, H. & Talik, E. X-ray investigation and discussion of the magnetostriction of Gd_3T (T = Ni, Rh, Ir_x) single crystals. *J. Appl. Cryst* **33**, 213–217 (2000).
16. Castilho, J. H., Chambouleyron, I., Marques, F. C., Rettori, C. & Alvarez, F. Electrical conductivity of amorphous silicon doped with rare-earth elements. *Phys. Rev. B* **43**, 8946–8950 (1991).

17. Hellman, F., Tran, M. Q., Gebala, A. E., Wilcox, E. M. & Dynes, R. C. Metal-insulator transition and giant negative magnetoresistance in amorphous magnetic rare earth silicon alloys. *Phys. Rev. Lett* **77**, 4652–4655 (1996).
18. Hellman, F., Queen, D. R., Potok, R. M. & Zink, B. L. Spin-glass freezing and RKKY interactions near the metal-insulator transition in amorphous Gd-Si alloys. *Phys. Rev. Lett* **84**, 5411–5414 (2000).
19. Mackintosh, A. R. Magnetic ordering and the electronic structure of rare-earth metals. *Phys. Rev. Lett* **9**, 90–93 (1962).
20. Yamada, H. & Takada, S. On the electrical resistivity of antiferromagnetic metals at low temperatures. *Prog. Theor. Phys* **52**, 1077–1093 (1974).
21. Mackintosh, A. R. & Spanel, L. E. Magnetoresistance in rare earth single crystals. *Solid State Commun* **2**, 383–386 (1964).
22. Yamada, H. & Takada, S. Magnetoresistance of antiferromagnetic metals due to *s-d* interactions. *J. Phys. Soc. Jpn* **34**, 51–57 (1973).
23. Jensen, J. & Mackintosh, A. R. *Rare Earth Magnetism: Structures and Excitations* (Clarendon Press, Oxford, 1991).
24. Molnr, S. & Stampe, P. A. *Magnetic polarons in "Handbook of magnetism and advanced magnetic materials"*. (John Wiley & Sons, Ltd, 2007).
25. Yosida, K. Anomalous electrical resistivity and magnetoresisitane due to an *s-d* interactin in Cu-Mn Alloys. *Phys. Rev* **107**, 396–403 (1957).
26. Bogach, A. V., Burkhanov, G. S., Chistyakov, O. D., Glushkov, V. V., Demishev, S. V., Samarin, N. A., Paderno, Yu. B., Shitsevalova, N. Yu. & Sluchanko, N. E. Bulk and local magnetization in $CeAl_6$ and CeB_6. *Physica B* **378**–**380**, 769–770 (2006).
27. Anisimov, M. A., Bogach, A. V., Glushkov, V. V., Demishev, S. V., Samarin, N. A., Shitsevalova, N. Yu & Sluchanko, N. E. Low temperature magnetotransport in RB_6 (R = Pr, Nd). *J. Phys.: Conf. Ser* **150**, 042005–4 (2009).
28. Mott, N. F. & Wills, H. H. The electrical conductivity of transition metals. *Proc. R. Soc. Lond. A* **153**, 699–717 (1936).
29. Wilson, A. H. The electrical conductivity of the transition metals. *Proc. R. Soc. Lond. A* **167**, 580–593 (1938).
30. Singh, D. J. Adequacy of the local-spin-density approximation for Gd. *Phys. Rev. B* **44**, 7451–7454 (1991).
31. Rodríguez-Carvajal, J. Recent advances in magnetic structure determination by neutron powder diffraction. *Physica B* **192**, 55–69 (1993).

Acknowledgements

H.F.L. thanks M.T. Fernandez-Diaz at Institut Laue-Langevin, France, for helpful discussions, and is grateful to E. Kentzinger at Forschungszentrum Jülich GmbH, Germany, for his efforts in keeping the high performance of the x-ray powder diffractometer. This work at RWTH Aachen University and Jülich Centre for Neutron Science JCNS Outstation at Institut Laue-Langevin was funded by the BMBF under contract No. 05K10PA3.

Author contributions

H.F.L., Y.X., B.S., J.P. and P.M. characterized the samples by Laue backscattering, temperature-dependent x-ray powder diffraction, SQUID, PPMS, etc. H.F.L., Y.X., W.S., G.R., and Th.B. discussed and analyzed the results. H.F.L led the project and wrote the paper.

Additional information

Supplementary Information accompanies this paper at http://www.nature.com/scientificreports

Competing financial interests: The authors declare no competing financial interests.

How to cite this article: Li, H. *et al*. Possible magnetic-polaron-switched positive and negative magnetoresistance in the GdSi single crystals. *Sci. Rep.* **2**, 750; DOI:10.1038/srep00750 (2012).